



AFRL-RY-WP-TR-2016-0206

**NONLINEAR ELASTICITY OF DOPED
SEMICONDUCTORS**

**Mark Dykman and Kirill Moskvovtsev
Michigan State University**

**FEBRUARY 2017
Final Report**

Approved for public release; distribution unlimited.

See additional restrictions described on inside pages

STINFO COPY

**AIR FORCE RESEARCH LABORATORY
SENSORS DIRECTORATE
WRIGHT-PATTERSON AIR FORCE BASE, OH 45433-7320
AIR FORCE MATERIEL COMMAND
UNITED STATES AIR FORCE**

NOTICE AND SIGNATURE PAGE

Using Government drawings, specifications, or other data included in this document for any purpose other than Government procurement does not in any way obligate the U.S. Government. The fact that the Government formulated or supplied the drawings, specifications, or other data does not license the holder or any other person or corporation; or convey any rights or permission to manufacture, use, or sell any patented invention that may relate to them.

This report is the result of contracted fundamental research deemed exempt from public affairs security and policy review in accordance with SAF/AQR memorandum dated 10 Dec 08 and AFRL/CA policy clarification memorandum dated 16 Jan 09. This report is available to the general public, including foreign nationals.

AFRL-RY-WP-TR-2016-0206 HAS BEEN REVIEWED AND IS APPROVED FOR PUBLICATION IN ACCORDANCE WITH ASSIGNED DISTRIBUTION STATEMENT.

// Signature//

LAVERN A STARMAN, Program Manager
Electro-Optical Components Branch
Aerospace Components & Subsystems Division

// Signature//

ATTILA A. SZEP, Acting Chief
Electro-Optical Components Branch
Aerospace Components & Subsystems Division

// Signature//

TODD W. BEARD, Lt Col, USAF
Aerospace Components & Subsystems Division
Sensors Directorate

This report is published in the interest of scientific and technical information exchange, and its publication does not constitute the Government's approval or disapproval of its ideas or findings.

*Disseminated copies will show “//Signature//” stamped or typed above the signature blocks.

REPORT DOCUMENTATION PAGE				Form Approved OMB No. 0704-0188	
The public reporting burden for this collection of information is estimated to average 1 hour per response, including the time for reviewing instructions, searching existing data sources, gathering and maintaining the data needed, and completing and reviewing the collection of information. Send comments regarding this burden estimate or any other aspect of this collection of information, including suggestions for reducing this burden, to Department of Defense, Washington Headquarters Services, Directorate for Information Operations and Reports (0704-0188), 1215 Jefferson Davis Highway, Suite 1204, Arlington, VA 22202-4302. Respondents should be aware that notwithstanding any other provision of law, no person shall be subject to any penalty for failing to comply with a collection of information if it does not display a currently valid OMB control number. PLEASE DO NOT RETURN YOUR FORM TO THE ABOVE ADDRESS.					
1. REPORT DATE (DD-MM-YY) February 2017		2. REPORT TYPE Final		3. DATES COVERED (From - To) 12 November 2015 – 12 November 2016	
4. TITLE AND SUBTITLE NONLINEAR ELASTICITY OF DOPED SEMICONDUCTORS				5a. CONTRACT NUMBER FA8650-16-1-7600	
				5b. GRANT NUMBER	
				5c. PROGRAM ELEMENT NUMBER 62716E	
6. AUTHOR(S) Mark Dykman and Kirill Moskovtsev				5d. PROJECT NUMBER DARPA	
				5e. TASK NUMBER N/A	
				5f. WORK UNIT NUMBER Y1EG	
7. PERFORMING ORGANIZATION NAME(S) AND ADDRESS(ES) Michigan State University 426 Auditorium Rd, Rm 2 East Lansing, MI 48824-2600				8. PERFORMING ORGANIZATION REPORT NUMBER	
9. SPONSORING/MONITORING AGENCY NAME(S) AND ADDRESS(ES) Air Force Research Laboratory Sensors Directorate Wright-Patterson Air Force Base, OH 45433-7320 Air Force Materiel Command United States Air Force				10. SPONSORING/MONITORING AGENCY ACRONYM(S) AFRL/RYPD	
				11. SPONSORING/MONITORING AGENCY REPORT NUMBER(S) AFRL-RY-WP-TR-2016-0206	
12. DISTRIBUTION/AVAILABILITY STATEMENT Approved for public release; distribution is unlimited.					
13. SUPPLEMENTARY NOTES This report is the result of contracted fundamental research deemed exempt from public affairs security and policy review in accordance with SAF/AQR memorandum dated 10 Dec 08 and AFRL/CA policy clarification memorandum dated 16 Jan 09. This material is based on research sponsored by Air Force Research Laboratory (AFRL) and the Defense Advanced Research Agency (DARPA) under agreement number FA8650-16-1-7600. The U.S. Government is authorized to reproduce and distribute reprints for Governmental purposes notwithstanding any copyright notation herein. The views and conclusions contained herein are those of the authors and should not be interpreted as necessarily representing the official policies of endorsements, either expressed or implied, of AFRL and the DARPA or the U.S. Government. Report contains color.					
14. ABSTRACT In this report Michigan State University (MSU) provides the results of studying the temperature dependence of the frequency shift and the amplitude dependence of the vibration frequency for <100> length extension modes in n-doped silicon (Si) microelectromechanical (MEMS) resonators. MSU also has started a comparison with the experimental data from the Stanford University group. The obtained results show that the goal of the project has been reached. MSU has full quantitative theory of the temperature- and density-dependent change of the vibration frequency of eigenmodes in resonators and of their dependence on the vibration amplitude.					
15. SUBJECT TERMS semiconductors, microresonators, microelectromechanical					
16. SECURITY CLASSIFICATION OF:			17. LIMITATION OF ABSTRACT: SAR	18. NUMBER OF PAGES 30	19a. NAME OF RESPONSIBLE PERSON (Monitor) Lavern Starman 19b. TELEPHONE NUMBER (Include Area Code) N/A
a. REPORT Unclassified	b. ABSTRACT Unclassified	c. THIS PAGE Unclassified			

Table of Contents

Section	Page
List of Figures	ii
1.0 MAJOR ACCOMPLISHMENTS	1
2.0 MAJOR FINDINGS	4
3.0 THE TEAM	6
APPENDIX A: STRONG VIBRATION NONLINEARITY IN SEMICONDUCTOR- BASED NANOMECHANICAL SYSTEMS	7
LIST OF ACRONYMS, ABBREVIATIONS, AND SYMBOLS	24

List of Figures

Figure	Page
Figure 1: Strain Shifts Valleys, Leading to a Population Difference	1
Figure 2: Si Brillouin Zone and Conduction Band Valleys.....	2
Figure 3: Two Types of Vibrational Modes in Microelectromechanical Systems (MEMS) used to calculate the Linear and Nonlinear Frequency Shift	4
Figure 4: Nonlinear Frequency Shift Scaled by the Squared Vibration Amplitude a_x^2 vs. Temperature in n-doped Si Lamé Resonators.....	5

1.0 MAJOR ACCOMPLISHMENTS

We have studied the temperature dependence of the frequency shift and the amplitude dependence of the vibration frequency for <100> length extension modes in n-doped silicon (Si) microelectromechanical (MEMS) resonators and have started a comparison with the experimental data from Kenny's group. The theoretical analysis is based on minimizing the free energy

$$F = F_e + F_v; F_e = \int d\mathbf{r} \left\{ \sum_{\alpha} f [n_{\alpha}(\mathbf{r})] + n_{\alpha}(\mathbf{r}) \Xi_{ik}^{\alpha} \varepsilon_{ik}(\mathbf{r}) \right\}, \quad (1)$$

over the electron densities $n_{\alpha}(\mathbf{r})$ in different valleys $\alpha = 1, 2, 3$ for a given strain $\varepsilon_{ik}(\mathbf{r})$ with the constraint that the total density remains constant, $\delta F / \delta n_{\alpha}(\mathbf{r}) = \mu$. Parameters Ξ_{ik}^{α} are the parameters of the deformation potential, with typical values $\sim 10\text{eV}$; F_v is the free energy of vibrations in the absence of electron-phonon coupling. The minimization applies where the rate of intervalley electron transitions largely exceeds the typical frequencies of the studied modes, which is the case in the experiment. The physical idea is that strain shifts the electron energy minima with respect to each other, making the populations of different minima different, as illustrated in Figure 1. In turn, the difference in the populations leads to stress.

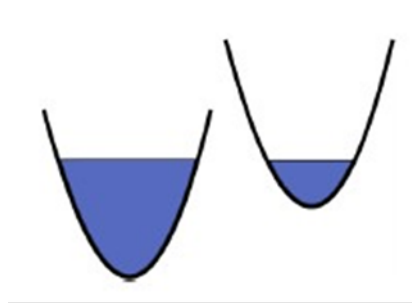


Figure 1: Strain Shifts Valleys, Leading to a Population Difference

The minimized electron free energy takes the form of a series expansion in the strain tensor,

$$\min F_e = \frac{1}{2} \widehat{\Lambda}_2 \widehat{\varepsilon} \widehat{\varepsilon} + \frac{1}{6} \widehat{\Lambda}_3 \widehat{\varepsilon} \widehat{\varepsilon} \widehat{\varepsilon} + \frac{1}{24} \widehat{\Lambda}_4 \widehat{\varepsilon} \widehat{\varepsilon} \widehat{\varepsilon} \widehat{\varepsilon} + \dots \quad (2)$$

Tensors $\widehat{\Lambda}_n$ are proportional to the electron density and to the parameter $(\Xi^{\alpha} / k_B T)^n$ with $n = 2, 3, 4$. This parameter is extremely large for room temperature and for the typical doping densities of 10^{19}cm^{-3} , reaching the value of order of $10^3 \gg 1$.

At the beginning of the project, the analysis was applied to <100> extensional modes, where tensor ε_{ik} has only diagonal components along the axes of the electron valleys and the coupling energy $\Xi_{ik}^{\alpha} \varepsilon_{ik}$ is nonzero. In the analysis we have also taken into account the internal nonlinearity of the crystal lattice, which leads to the temperature dependence of the mode frequencies even in the absence of the electron-phonon coupling. This effect is additive in terms

of the frequency shift, as seen from the expression for the free energy. The quartic in $\hat{\epsilon}$ term of internal nonlinearity (in energy) is small compared to the electron-phonon coupling induced nonlinearity, and therefore it may be disregarded in calculating the nonlinear frequency shift.

In the second quarter, we extended the results to $\langle 110 \rangle$ modes. In these modes, strain tensor has nonzero off-diagonal (shear) components. A *major extension* of the project is that we have started exploring the effective two-phonon coupling that results from the phonon-induced anticrossing of the bands. In silicon, in the conventionally used effective mass approximation there is no linear coupling between shear strain and conduction electrons. However, shear strain has pronounced effects on the electronic structure beyond this approximation. It comes primarily from the vicinity of the degeneracy (Dirac-type) point in the band structure, where two electron energy bands intersect. This is point X on the boundary of the Brillouin zone shown in Figure 2 below.

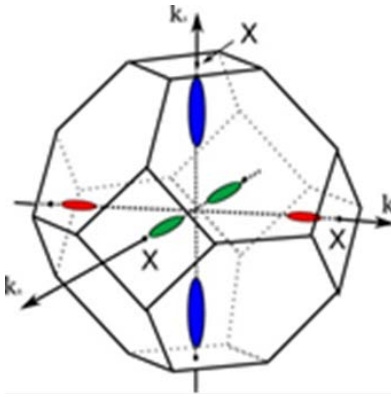


Figure 2: Si Brillouin Zone and Conduction Band Valleys

The Hamiltonian around point X along the kz axis is written as:

$$H_X = I\lambda + \sigma_x(A_3k_xk_y + \Xi_3\varepsilon_{xy}) + A_4\sigma_zk_z \quad (3)$$

Here,

$$\lambda = A_1k_z^2 + A_2(k_x^2 + k_y^2) + \Xi_1\varepsilon_{zz} + \Xi_2(\varepsilon_{xx} + \varepsilon_{yy}) \quad (4)$$

As a result, the k_z - valley's bottom shifts quadratically with shear strain:

$$\Delta E(z) = -\frac{\Xi_3^2}{\delta E}\varepsilon_{xy}^2 \quad (5)$$

where δE is the splitting of the energy bands at the positions of the valleys. A similar expression applies to other valleys. Effectively, this result is equivalent to a two-phonon coupling. Incorporating this effect into the model described above makes it possible to calculate the effects

of the shear electron-phonon coupling on the linear and nonlinear elasticity for $\langle 110 \rangle$ modes. This is a major endeavor, and the calculations are at the early stage.

In the third quarter we have performed detailed calculations of the two-phonon coupling due to shear strain. We have shown how it affects the temperature dependence of the mode frequencies and the mode nonlinearity, including the dependence of the mode frequency on the vibration amplitude. We have also started a comparison of the results with the experiments from the Kenny group on the frequency dependence on the temperature and the amplitude.

In the fourth quarter we have summarized the results in a paper, which is included as Appendix A, and have developed a code that is publicly available at:

http://www.pa.msu.edu/people/dykman/nonlinear_elasticity

This code allows calculating the temperature dependent corrections to the frequency due to the doping and the nonlinear frequency shift due to finite vibration amplitude in Si resonators for different types of modes. The code provides both the analytical expressions and evaluates them numerically using the parameters. It also allows finding the doping-induced corrections to linear and nonlinear elasticity in germanium (Ge).

2.0 MAJOR FINDINGS

- Fully analyzed the effect of the degeneracy of the conduction bands at the points X of the Brillouin zone on the mode nonlinearity and the temperature dependent frequency shift due to the doping. The analysis goes beyond the conventional deformation potential approximation and is necessary to describe the coupling to shear strain modes.
- Tested the theory against the existing in the literature experimental data on the effect of doping on the speed of transverse sound and the hitherto unexplained effect of uniaxial stress on the speed of sound in the geometry where the deformation potential does not lead to such an effect.
- In collaboration with Kenny's group, obtained new experimental data on the doping- induced temperature dependence of the frequency and on the nonlinearity of the $\langle 110 \rangle$ and $\langle 100 \rangle$ Lamé modes.
- Described the experimental data on the temperature and amplitude dependence of the frequency of the Lamé modes in Si microresonators. The results describe the experimental observations on the anomalous *softening* nonlinearity in the $\langle 110 \rangle$ modes, which behaves monotonically with doping density, as opposed to the *hardening* nonlinearity in the $\langle 100 \rangle$ modes which behaves in a non-monotonic way with doping density.
- Developed a symbolic and numerical codes to evaluate the effects for different modes in Si and Ge microresonators.

The modes used in the simulations of Si resonators are shown in Figure 3. The results of a comparison of the theory with the experimental data on the nonlinear frequency shift of the Lamé modes in Si microresonators are shown in Figure 4. The comparison is performed for two donor densities. The data refer to two types of modes. One mode is coupled to the electron density via deformation potential (the Lamé mode in a plate cut along the $\langle 100 \rangle$ axes). The other mode refers to the plate cut along $\langle 110 \rangle$ axes, where the displacement field is pure shear and the coupling to the electron density is through the band splitting at the X points of the Brillouin zone.

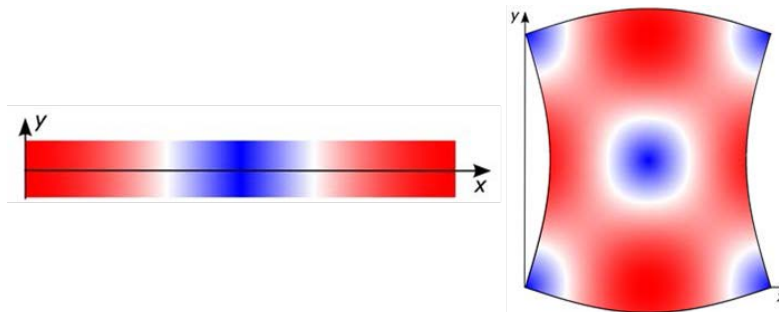


Figure 3: Two Types of Vibrational Modes in Microelectromechanical Systems (MEMS) used to calculate the Linear and Nonlinear Frequency Shift

Left panel: Length extension mode in the $\langle 110 \rangle$ direction in a thin narrow resonator. Right panel: Lamé mode in a thin plate resonator with the sides along $\langle 110 \rangle$.

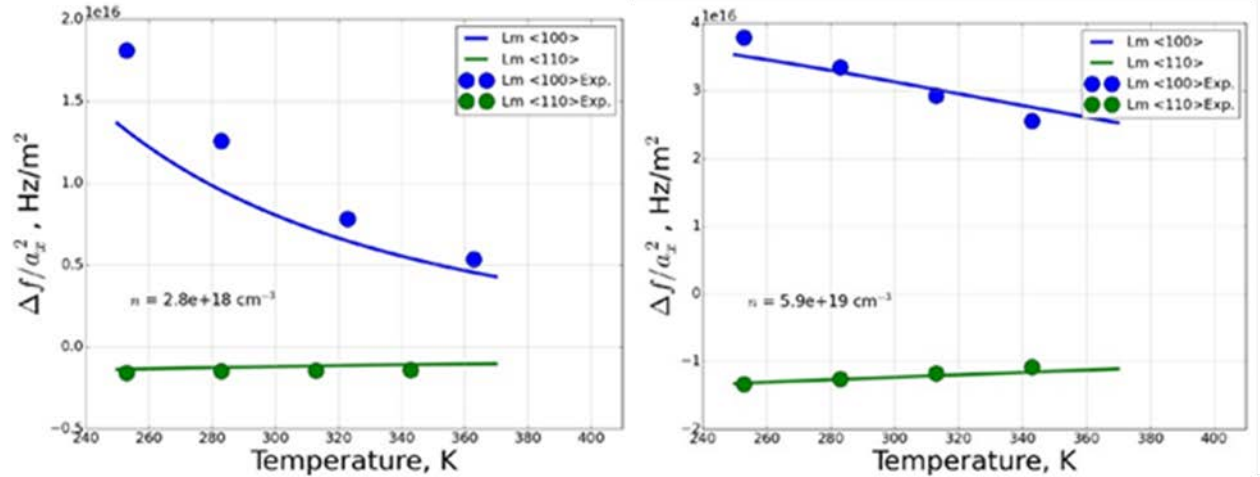


Figure 4: Nonlinear Frequency Shift Scaled by the Squared Vibration Amplitude a_x^2 vs. Temperature in n-doped Si Lamé Resonators

Solid lines show the present theory. Dots: experimental points obtained by the group of T. Kenny. The experimental values of the amplitude are obtained assuming the gap between the resonator and the electrodes to be $1.1 \mu\text{m}$ in the absence of vibrations. The donor density in the left panel is: $n = 2.8 \times 10^{18} \text{ cm}^{-3}$; in the right panel $n = 5.9 \times 10^{19} \text{ cm}^{-3}$.

The theory has no adjustable parameters and is in an excellent agreement with the experiment.

The obtained results show that the goal of the project has been reached. We have full quantitative theory of the temperature- and density-dependent change of the vibration frequency of eigenmodes in resonators and of their dependence on the vibration amplitude.

3.0 THE TEAM

The work was done at Michigan State University. The principal investigators were Mark Dykman and Steven Shaw. The graduate student was Kirill Moskovtsev. The work was done in close cooperation with the team of Thomas Kenny at Stanford University.

APPENDIX A: STRONG VIBRATION NONLINEARITY IN SEMICONDUCTOR-BASED NANOMECHANICAL SYSTEMS

Kirill Moskovtsev¹ and M. I. Dykman¹

¹Department of Physics and Astronomy, Michigan State University, East Lansing, Michigan 48824, USA

(Dated: November 28, 2016)

We study the effect of the electron-phonon coupling on vibrational eigenmodes of nano- and micro-mechanical systems made of semiconductors with equivalent energy valleys. We show that the coupling can lead to a strong mode nonlinearity. The mechanism is the lifting of the valley degeneracy by the strain. The redistribution of the electrons between the valleys is controlled by a large ratio of the electron-phonon coupling constant to the electron chemical potential or temperature. We find the quartic in the strain terms in the electron free energy, which determine the amplitude dependence of the mode frequencies. This dependence is calculated for silicon micro- systems. It is significantly different for different modes and the crystal orientation, and can vary nonmonotonously with the electron density and temperature.

I. Introduction

The electron-phonon coupling strongly affects vibrational modes of nano- and micro-electro-mechanical systems. Much interest have attracted the effects of this coupling related to the reduced dimensionality of the electron system, as they make it possible to reveal interesting consequences of the electron correlations at the nanoscale, the Coulomb blockade being a simple example, cf. [1–9] and references therein.

Much less attention has been paid to the consequences of the electron-phonon coupling, which are related to the discreteness of the vibrational spectrum of a nanosystem, but emerge in the absence of size quantization of the electron motion. One of such consequences, which we study in this paper, is the coupling-induced change of the vibration nonlinearity. Strong nonlinearity is a generic feature of vibrations in small systems [10, 11]. Its easily accessible manifestation is the dependence of the mode frequencies on the vibration amplitudes. This dependence corresponds to the “self-action” of the mode, and its familiar analog in bulk crystals are acoustic solitons [12, 13]; however, the nonlinearity required for observing such solitons usually is sufficiently strong only for high-frequency phonons. Also, the change of the eigen frequency with the mode amplitude is of interest for modes with a discrete frequency spectrum, such as standing waves in mesoscopic systems, but not for propagating waves with a quasi-continuous spectrum.

Much attention have been recently attracting Si-based nano- and micromechanical systems, see [14, 15] and references therein. In such systems there was observed an unexpectedly large change of the amplitude dependence of the vibration frequency with the varying electron density [16, 17]. When the doping level was increased from $2.8 \times 10^{18} \text{ cm}^{-3}$ to $5.9 \times 10^{19} \text{ cm}^{-3}$, the nonlinearity parameter increased by more than an order of magnitude. Moreover, the nonlinearity change was different for the vibrational modes with different spatial structure. In this paper we develop a theory of the nonlinearity of vibrational modes in semiconductor nano- and micro-mechanical systems with high electron density. We show that the electron-phonon coupling can lead to a strong self-action of the vibrational modes, which in turn significantly modifies the

amplitude dependence of the mode frequencies. We find the dependence of the effect on the electron density and temperature.

For bulk semiconductors, the effect of the electron-phonon coupling on the elastic properties, including the three-phonon coupling, was first analyzed by Keyes [18]. The analysis referred to n -Ge and was based on the deformation potential approximation. The idea was that deformation lifts the degeneracy of the equivalent electron valleys, which leads to a redistribution of the electrons over the valleys. In turn, such redistribution changes the speed of sound depending on the direction and polarization of the sound waves and also affects the sound speed in the presence of uniaxial stress. This theory was extended to silicon and the corresponding measurements were done by Hall [19]. However, Hall also observed the change of the speed of transverse sound waves and the effect of stress on sound propagation in the geometries, where these effects are due to shear deformation and do not arise in the deformation potential model. A theory of the change of the linear shear elastic constant in silicon due to the intervalley redistribution of the electrons was developed by Cerdeira and Cardona [20].

As we show, in mesoscopic systems the strain-induced redistribution of the electrons over the valleys of the conduction band leads to the previously unexplored strong fourth-order nonlinearity of the vibrational modes. This nonlinearity gives a major contribution to the amplitude dependence of the vibration frequency. The redistribution also leads to a temperature dependence of the frequencies. The magnitudes of the effects sensitively depends on the mode structure. We describe them for several types of modes, including those studied in the experiment [16, 17] and qualitatively compare the results with the observations. The theoretical results refer to both degenerate and nondegenerate electron systems. Specific calculations are done for silicon resonators.

In Sec. II we give, for completeness, the expressions for the mode normalization and the amplitude-dependent frequency shift of coupled nonlinear modes in a nano- or micro-system. In Sec. III and Appendix A we provide expressions for the electron-phonon coupling induced change of the elasticity parameters, including the parameters of quartic nonlinearity. In Sec. IV we discuss the asymptotic behavior of the parameters of quartic nonlinearity for low and high electron density and give their explicit form for silicon. In Sec. V we calculate the nonlinear frequency shift for several frequently used vibrational modes in single-crystal silicon systems and show the dependence of this shift on the electron density and temperature. The explicit analytical expressions are given in Appendices C and D. Sec. VI contains concluding remarks.

II. Nonlinear Frequency Shift of Low-Frequency Eigenmodes

Of primary interest for nano- and micro-mechanical systems are comparatively low-frequency modes with wavelength on the order of the maximal size of the system. Examples are provided by long-wavelength flexural modes of nanotubes, nanobeams, and nano/micro-membranes, or acoustic-type modes in microplates or beams. These modes are easy to excite and detect. We will enumerate them by index ν . Their dynamics is described by the elasticity theory [21]. The spatial structure of the displacement field of a mode $\mathbf{u}^{(\nu)}(\mathbf{r})$ in the harmonic approximation is determined by the boundary conditions. We will choose $\mathbf{u}^{(\nu)}(\mathbf{r})$ dimensionless, so that in our finite-size system

$$\int d\mathbf{r} \mathbf{u}^{(\nu)}(\mathbf{r}) \cdot \mathbf{u}^{(\nu')}(\mathbf{r}) = V \delta_{\nu\nu'}. \quad (1)$$

Here, V is the volume of the system. We assumed that the mode eigenfrequencies ω_ν are nondegenerate; including degenerate modes is straightforward. For simplicity, we also assumed that the system is spatially uniform; an extension to spatially nonuniform systems is straightforward as well.

We emphasize the distinction of the normalization (1) from the conventional normalization for bulk crystals, where ν corresponds to the wave vector and the branch number, and the normalization integral is independent of the volume. The normalization (1) is convenient for the analysis of low-frequency modes with the discrete spectrum characteristic of mesoscopic systems. Such modes are standing waves, and therefore vectors $\mathbf{u}^{(\nu)}$ can be chosen real.

The low-frequency part of the displacement can be written as

$$\mathbf{u}(\mathbf{r}, t) = \sum_{\nu} Q_{\nu}(t) \mathbf{u}^{(\nu)}(\mathbf{r}). \quad (2)$$

Functions $Q_{\nu}(t)$ give the mode amplitudes. In the harmonic approximation the dynamics of the standing waves is described by the Hamiltonian

$$H_h = \frac{1}{2} \sum_{\nu} (M^{-1} P_{\nu}^2 + M \omega_{\nu}^2 Q_{\nu}^2), \quad (3)$$

where P_{ν} is the momentum of mode ν and M is the mass of the system.

The anharmonicity of the crystal leads to mode-mode coupling. Within the elasticity theory this coupling is described by the terms in the Hamiltonian, which are cubic and quartic in the strain tensor. We will not consider higher-order terms, which are small for the mode amplitudes of interest. From the expansion (2), we obtain the nonlinear part of the Hamiltonian in the form

$$H_{nl} = \frac{1}{3} \sum \beta_{\nu_1 \nu_2 \nu_3} Q_{\nu_1} Q_{\nu_2} Q_{\nu_3} + \frac{1}{4} \sum \gamma_{\nu_1 \nu_2 \nu_3 \nu_4} Q_{\nu_1} Q_{\nu_2} Q_{\nu_3} Q_{\nu_4}. \quad (4)$$

Equation (4) is essentially an expansion in the ratio of the mode amplitudes to their characteristic wavelength, which is of the order of the appropriate linear dimension of the system. This is why mesoscopic systems are of particular interest, as here vibrations of low-frequency eigenmodes become nonlinear for already small vibration amplitudes.

A familiar consequence of nonlinearity in nano- and micromechanical systems is the dependence of the vibration frequency of a mode on its own amplitude and on the amplitudes of other modes,

see Ref. 11 for a review. In particular, the change $\delta\omega_\nu$ of the mode frequency due to the vibrations of the mode itself, $Q_\nu(t) = A_\nu \cos \omega_\nu t$, is [22, 23]

$$\delta\omega_\nu \approx \left[\frac{3\gamma_\nu}{8M\omega_\nu} - \sum_{\nu'} \frac{\beta_{\nu\nu\nu'}^2(3\omega_{\nu'}^2 - 8\omega_\nu^2)}{4M^2\omega_\nu^3(\omega_{\nu'}^2 - 4\omega_\nu^2)} \right] A_\nu^2, \quad (5)$$

where $\gamma_\nu \equiv \gamma_{\nu\nu\nu}$ and we kept the terms of the first order in γ and the second order in β .

The nonlinear mode coupling (4) leads also to the frequency shift due to thermal vibrations of the modes. The dominating contribution to this shift for low-frequency modes comes from their coupling to modes with frequencies $\sim k_B T/\hbar$, which have a much higher density of states. This shift is described by an expression that is similar to Eq. (5) with A_ν^2 replaced by $A_{\nu'}^2 \sim k_B T/M\omega_{\nu'}^2$, and placed under the sum over ν' , in the classical limit.

III. The Nonlinearity Due to the Electron-Phonon Coupling

We will consider the vibration nonlinearity due to the electron-phonon coupling in multi-valley semiconductors with cubic symmetry, silicon and germanium being the best known examples. In such semiconductors, the energy valleys of the conduction band are located at high-symmetry axes of the Brillouin zone. Strain lifts the symmetry and thus the degeneracy of the valleys.

The simplest mechanism of the electron-phonon coupling is the deformation potential. Here, the energy shift δE_α of valley α is determined by the deformation potential parameters Ξ_u and Ξ_d of the coupling to a uniaxial strain along the symmetry axis of the valley and to dilatation, respectively. In terms of the strain tensor ε_{ij} we have $\delta E_\alpha = \sum_{ij} \Xi_{ij}^{(\alpha)} \varepsilon_{ji}$, where $\hat{\Xi}^{(\alpha)} = \Xi_d \hat{I} + \Xi_u \mathbf{e}^{(\alpha)} \otimes \mathbf{e}^{(\alpha)}$, with $\mathbf{e}^{(\alpha)}$ being the unit vector along the symmetry axis of the valley. We use the hat symbol to indicate tensors and symbol “ \otimes ” to indicate tensor products. The analysis below is not limited to the deformation potential approximation. An important extension will be discussed using silicon as an example.

We assume that the strain varies in time and space slowly compared to the reciprocal rate of intervalley electron scattering and the intervalley scattering length, respectively. Then the electron system follows the strain adiabatically. The electron density $n^{(\alpha)}(\mathbf{r})$ in valley α is decreased or increased depending on whether the bottom of the valley goes up or down. In the single-electron approximation and for the deformation potential coupling, the electron free energy density for a given strain is $F_e = \sum_\alpha \{f_e[n^{(\alpha)}(\mathbf{r})] + n^{(\alpha)}(\mathbf{r}) \Xi_{ij}^{(\alpha)} \varepsilon_{ji}(\mathbf{r})\}$ where $f_e[n(\mathbf{r})]$ is the free energy density for electrons with density $n(\mathbf{r})$ in a valley in the absence of coupling to phonons.

The electro-neutrality requires that the total electron density summed over the valleys be constant. The free energy density F_e has to be minimized over $n^{(\alpha)}(\mathbf{r})$ to meet this constraint. This gives the change of the electron chemical potential $\delta\mu$ due to strain $\hat{\varepsilon}$. The resulting increment of the electron free energy density has the form of a series expansion in the strain tensor,

$$\begin{aligned} \delta F_e = & \widehat{\Lambda}_1 \cdot \widehat{\varepsilon} + \frac{1}{2} \widehat{\Lambda}_2 \cdot \widehat{\varepsilon} \otimes \widehat{\varepsilon} + \frac{1}{6} \widehat{\Lambda}_3 \cdot \widehat{\varepsilon} \otimes \widehat{\varepsilon} \otimes \widehat{\varepsilon} \\ & + \frac{1}{24} \widehat{\Lambda}_4 \cdot \widehat{\varepsilon} \otimes \widehat{\varepsilon} \otimes \widehat{\varepsilon} \otimes \widehat{\varepsilon} + \dots \end{aligned} \quad (6)$$

Here $\widehat{\Lambda}_1$, $\widehat{\Lambda}_2$, $\widehat{\Lambda}_3$, and $\widehat{\Lambda}_4$ are tensors of ranks 2, 4, 6, and 8, respectively. They are contracted with the tensor products of the strain tensor $\widehat{\varepsilon}$. Respectively, $\widehat{\Lambda}_k$ are the electronic contributions to the linear (for $k = 2$) and nonlinear (for $k > 2$) elasticity parameters of the crystal. These contributions are isothermal, but since the change of the mode frequencies from the electron-phonon coupling is small and the nonlinearity is also small, the difference with the adiabatic expressions can be disregarded.

To the third order in $\widehat{\varepsilon}$ the expression for δF_e in terms of the shift of the valleys was found by Keyes [18] in the analysis of sound wave propagation. However, to find the parameters of the quartic nonlinearity of resonant modes in small systems, which is of primary interest to us, we also need to keep quartic terms in Eq. (6).

As seen from the explicit form of the parameters of the expansion (6) given in Appendix A, $\widehat{\Lambda}_k \propto \Xi_u [\Xi_u / \max(\mu_0, k_B T)]^{k-1}$ $k = 1, 2, \dots$, where μ_0 is the electron chemical potential in the absence of strain; it is determined by the total (summed over the valleys) electron density n . Of central importance for the analysis is that parameter $\Xi_u / \max(\mu_0, k_B T) \sim 10^3$ for electron densities $n \sim 10^{19} \text{ cm}^{-3}$ and room temperatures, i.e.

$$\Xi_u / \max(\mu_0, k_B T) \gg 1. \quad (7)$$

As a consequence, the coefficients at the nonlinear in $\widehat{\varepsilon}$ terms in Eq. (6) quickly increase with the increasing order of the nonlinearity [the overall series (6) is converging fast because of the smallness of the strain tensor].

The increase of $\widehat{\Lambda}_k$ with k allows us to keep in $\widehat{\varepsilon}$ only the terms linear in the lattice displacement, i.e., to set $\varepsilon_{ij} = (1/2)(\partial u_i / \partial x_j + \partial u_j / \partial x_i)$, where u_i and x_i are the components of the displacement and the coordinates, respectively. Indeed, in this case a k th term of the series (6) is of order k in the displacement. If we included the quadratic in $\partial u_i / \partial x_j$ term into one of the $\widehat{\varepsilon}$ tensors in the k th term, this term would become of order $k + 1$ in the displacement. However, for linear $\widehat{\varepsilon}$ the $(k + 1)$ th term in the series (6) is also of the $(k + 1)$ th order in the displacement, but is larger by factor $\Xi_u / \max(\mu_0, k_B T)$.

For linear $\widehat{\varepsilon}$, the total strain is a sum of partial contributions of strain from individual modes. For mode ν , such partial contribution is expressed in terms of the scaled displacement $\mathbf{u}^{(\nu)}(\mathbf{r})$ [see Eq. (2)] as $\widehat{\varepsilon} = Q_\nu \varepsilon^{(\nu)}$, where $\varepsilon_{ij}^{(\nu)}(\mathbf{r}) = \frac{1}{2} [\partial u_i^{(\nu)}(\mathbf{r}) / \partial x_j + \partial u_j^{(\nu)}(\mathbf{r}) / \partial x_i]$. We note that, in contrast to the dimensionless strain tensor $\widehat{\varepsilon}$, tensor $\varepsilon^{(\nu)}$ has dimension [length] $^{-1}$.

From Eq. (6) we find the electronic contributions to the nonlinearity parameters $\beta_{\nu_1 \nu_2 \nu_3}^{(e)}$, $\gamma_{\nu_1 \nu_2 \nu_3 \nu_4}^{(e)}$ in Hamiltonian (4),

$$\begin{aligned}\beta_{\nu_1\nu_2\nu_3}^{(e)} &= \frac{1}{2} \int d\mathbf{r} \hat{\Lambda}_3 \cdot \hat{\varepsilon}^{(\nu_1)} \otimes \hat{\varepsilon}^{(\nu_2)} \otimes \hat{\varepsilon}^{(\nu_3)}, \\ \gamma_{\nu_1\nu_2\nu_3\nu_4}^{(e)} &= \frac{1}{6} \int d\mathbf{r} \hat{\Lambda}_4 \cdot \hat{\varepsilon}^{(\nu_1)} \otimes \hat{\varepsilon}^{(\nu_2)} \otimes \hat{\varepsilon}^{(\nu_3)} \otimes \hat{\varepsilon}^{(\nu_4)},\end{aligned}\quad (8)$$

where $\hat{\varepsilon}^{(\nu)} \equiv \hat{\varepsilon}^{(\nu)}(\mathbf{r})$; tensors $\hat{\Lambda}_k$ are independent of \mathbf{r} . Similarly, the electronic contribution to the eigenfrequency is

$$\Delta\omega_\nu^{(e)} = \frac{1}{2M\omega_\nu} \int d\mathbf{r} \hat{\Lambda}_2 \cdot \hat{\varepsilon}^{(\nu)} \otimes \hat{\varepsilon}^{(\nu)}. \quad (9)$$

Generally the term $\propto \hat{\Lambda}_2$ leads to mode mixing; however, if the mode frequencies are nondegenerate, this mixing is weak and can be disregarded, to the leading order in the electron-phonon coupling. One can see that the effect of the static stress $\propto \hat{\Lambda}_1$ can be disregarded as well.

The frequency change (9) depends on temperature because of the temperature dependence of $\propto \hat{\Lambda}_2$. The nonlinearity (8) also leads to a temperature dependence of the mode eigenfrequency. Together they modify the temperature dependence of the mode eigenfrequencies compared to that of undoped crystals. This modification often weakens the temperature dependence of the eigenfrequencies, which proves very important for applications of micro-mechanical systems in devices that work in a broad temperature range [24].

Equations (6)-(9) are generic and apply beyond the deformation potential approximation. This is of particular importance for silicon. Here, the electron band valleys lie on the $\langle 100 \rangle$ -axes close to the X -points on the zone boundaries where two electron energy bands cross. Lattice strain can lead to a band splitting at X -points and a shift of the valleys [25, 26]. Importantly, this shift results from a shear strain, which does not lead to a linear in the strain shift in the deformation potential approximation. The valley shift is quadratic in $\hat{\varepsilon}$ in this case, as explained in Appendix A, which corresponds to an effectively two-phonon coupling. The coupling parameter Ξ_{sh} is quadratic in the strain-induced band splitting, see Eq. (A2). It is large, much larger than the constant Ξ_u . Therefore the arguments given below Eq. (7) apply in this case as well. For purely shear strain in silicon, terms of odd order in $\hat{\varepsilon}$ in δF_e , Eq. (6), vanish.

IV. Explicit Form of the Tensors of Nonlinear Elasticity

Tensors $\hat{\Lambda}_n$ can be obtained by minimizing the free energy density of the electron system for a given strain and expanding the result in a series in $\hat{\varepsilon}$. A general procedure that allows one to find the components $\hat{\Lambda}_n$ for $n \leq 4$ is described in Appendix A. Using the symmetry arguments, the elasticity tensors are conveniently written in the contracted (Voigt) notation where the symmetric strain tensor is associated with a six-component vector. Then the nonlinear elasticity tensors $\hat{\Lambda}_3$ and $\hat{\Lambda}_4$ become tensors of rank three and four in the corresponding vector space. We use

notation $\delta\hat{c}$ for tensors $\hat{\Lambda}$ in these notations to emphasize that we are calculating corrections to the nonlinear elasticity tensors due to the electron-phonon coupling.

The explicit expressions for the nonlinear elasticity tensors $\delta\hat{c}$ are given in Table I. They refer to silicon and include the contributions that come from both the deformation potential coupling and from the splitting of the electron bands due to shear strain. In the deformation potential approximation, the components of the third-rank tensor $\delta\hat{c}$, which determine the cubic in the strain terms in the free energy, were found earlier [19]. Therefore we give only the components that contain a contribution from shear strain.

The fourth-rank tensor $\delta\hat{c}$ determines the quartic in the strain terms in the free energy and has not been discussed before, to the best of our knowledge. We give all independent components of this tensor. It is expressed in terms of the derivative of the electron density n over the chemical potential in the absence of strain μ_0 , which is a familiar thermodynamic characteristic. It is intuitively clear that the considered effect of the change of the electron density in different valleys in response to strain should be related to the derivative $dn/d\mu_0$. Interestingly because we consider nonlinear response to strain, the expressions in Table I contain also higher-order derivatives of n over μ_0 . As we will see, this leads to a nontrivial behavior of the nonlinear frequency shift with varying temperature and density. The considered mechanism of the strain-induced inter-valley electron redistribution does not contribute to the components c_{1123} and c_{1456} , therefore $\delta c_{1123} = \delta c_{1456} = 0$.

A. Nonlinear Elasticity in the Limiting Cases

The expressions for $\delta\hat{c}$ simplify in the case of low doping (or high temperature), where the electron gas is strongly nondegenerate, and in the opposite case of a strongly degenerate electron gas. For a nondegenerate gas, where the chemical potential in the absence of strain is $\mu_0 < 0$, $|\mu_0| \gg k_B T$, we have in Table I $F_{1/2}(x) = \frac{1}{4}\pi^{1/2}e^x$ with $x = \mu_0/k_B T$. The μ_0 -dependent factors $\exp(\mu_0/k_B T)$ in $F_{1/2}$ and its derivatives cancel each other in the expressions for $\delta\hat{c}$ and drop out from these expressions. The dependence of $\delta\hat{c}$ on density is then just linear, $\delta\hat{c} \propto n$. Parameters $C_{1,\dots,4}$ in Table I depend only on temperature, $C_1 \propto T^{-1}$, $C_2 \propto T^{-3}$, $C_3 \propto T^{-2}$ and $C_4 \propto T^{-1}$.

The decrease of the nonlinear elasticity parameters with increasing temperature in a nondegenerate electron gas is easy to understand. The effect we consider is determined by the competition between the energetically favorable unequal population of the electron energy valleys in a strained crystal and the entropically more favorable equal valley population. With increasing temperature the entropic factor becomes stronger, leading to a smaller population difference and thus smaller effect of the electron system on the vibrations.

For strong doping, where $\mu_0/k_B T \gg 1$, we have $\mu_0 \propto n^{2/3}$, and then $F_{1/2}(x) \approx \frac{2}{3}x^{3/2}$ with $x = \mu_0/k_B T$. Therefore parameters $C_{1,\dots,4}$ in Table I become temperature independent, with $nC_1 \propto n^{1/3}$, $nC_2 \propto n^{-1}$, $nC_3 \propto n^{-1/3}$, and $nC_4 \propto n^{1/3}$.

The results on the asymptotic behavior of the corrections to nonlinear elasticity are not limited to silicon. Since parameters $C_{1,2,3,4}$ are given by the coefficients in the general expansion of the free energy in strain, (A1), these results can be applied to the nonlinear elasticity induced by the electron-phonon coupling in other multi-valley semiconductors. To illustrate this point, in Appendix B we give $\delta\hat{c}$ tensor in germanium.

The difference between the asymptotic behavior of the tensors $\delta\hat{c}$ in the limits of nondegenerate and strongly degenerate electron gas can lead to a peculiar density and temperature dependence of the nonlinear frequency shift of the vibrational modes. It comes from the coefficients $C_{1,\dots,4}$ containing higher-order derivatives of n with respect to μ_0 . In the transition region $\mu_0 \sim k_B T$, thinking of the competition between the entropic and energetic factors does not provide a simple insight into the behavior of $\delta\hat{c}$, as both the energy and the entropy are complicated functions of density and temperature.

TABLE I. The change of the components of the nonlinear elasticity tensors due to the strain-induced electron redistribution between equivalent energy valleys in doped silicon. The coordinate axes are chosen along the $\langle 100 \rangle$ axes. Parameter Ξ_{sh} characterizes the effectively two-phonon coupling to shear strain. This parameter as well as function $F_{1/2}(x)$ are defined in Appendix A; $x = \mu_0/k_B T$ and n is the electron density.

$\delta c_{144} = -2\delta c_{155}$	$\frac{1}{9}n\Xi_u\Xi_{\text{sh}}C_1$	$C_1 = F'_{1/2}/F_{1/2}k_B T = d \ln n / d\mu_0$
$\delta c_{1111} = -2\delta c_{1112} = 2\delta c_{1122}$	$\frac{2}{27}n\Xi_u^4 C_2$	$C_2 = (k_B T)^{-3} F_{1/2}'^2 [d^2(1/F_{1/2}')/dx^2] / F_{1/2}$ $= (dn/d\mu_0)^2 [d^2(d\mu_0/dn)/d\mu_0^2] / n$
$\delta c_{1144} = -2\delta c_{1155} = -2\delta c_{1244} = \delta c_{1266}$	$-\frac{1}{27}n\Xi_u^2\Xi_{\text{sh}}C_3$	$C_3 = F_{1/2}''/F_{1/2}(k_B T)^2 = n^{-1}d^2n/d\mu_0^2$
$\delta c_{4444} = -6\delta c_{4455}$	$-\frac{1}{6}n\Xi_{\text{sh}}^2 C_4$	$C_4 = F'_{1/2}/F_{1/2}k_B T = d \ln n / d\mu_0$

V. Doping-Induced Nonlinearity of Simple Vibrational Modes

The nonlinear elasticity tensors in Table I give the doping-induced contributions to the nonlinearity parameters of the eigenmodes of micro- and nano-mechanical systems. These contributions are described by Eq. (8). As mentioned before, an important characteristic of the mode nonlinearity is the dependence of the mode frequency on the vibration amplitude. To the leading order, it is given by Eq. (5). This dependence has a contribution from the nonlinearity of an undoped crystal, which is quadratic in the parameters of the cubic nonlinearity; for example, if the latter is described by the Grüneisen constant, the corresponding contribution is quadratic in this constant. It is typically small. There is also a contribution from the quartic nonlinearity; the parameters of such nonlinearity are not known in undoped crystals and are not expected to be large. Respectively, the amplitude dependence of the vibration frequency for low-frequency modes in weakly doped single-crystal micro-mechanical systems is relatively weak [17].

A feature of the doping-induced nonlinearity described by Table I is that the quartic in the strain term in the free energy has a large coefficient compared to the cubic term, cf. Eq. (7) and the discussion below this equation. Therefore, in Eq. (5) for the amplitude dependence of vibration

frequency one can keep only the Duffing non-linearity constant γ_ν . The contribution from the cubic nonlinearity terms $\propto \beta_{\nu\nu\nu}^2$ can be disregarded. For a mode ν , the doping-induced contribution to γ_ν is equal to $\gamma_{\nu\nu\nu\nu}^{(e)}$ in Eq. (8).

To find the dependence of the mode frequency on the vibration amplitude we go through the following steps. First, we find the normal modes of interest for the given geometry of the system, with account taken of the boundary conditions, and normalize the displacements $\mathbf{u}^{(\nu)}(\mathbf{r})$ as indicated in Eq. (1). We use $\mathbf{u}^{(\nu)}(\mathbf{r})$ to find the strain tensor $\hat{\varepsilon}^{(\nu)}(\mathbf{r})$. The result is substituted into Eq. (8) and is convoluted with tensor $\hat{\Lambda}_4$, giving the value of γ_ν which is then used in Eq. (5) to find the frequency dependence on the vibration amplitude $\delta\omega_\nu$. Of particular interest is the relative frequency shift $\delta\omega_\nu/\omega_\nu$. To find this shift to the leading order, one can disregard nonlinearity when calculating the eigenfrequency ω_ν . Then, from Eq. (5),

$$\frac{\delta\omega_\nu}{\omega_\nu} = \frac{3\gamma_\nu A_\nu^2}{8 \int d\mathbf{r} \hat{\Lambda}_2^{(f)} \cdot \hat{\varepsilon}^{(\nu)} \otimes \hat{\varepsilon}^{(\nu)}}, \quad (10)$$

where $\hat{\Lambda}_2^{(f)}$ is the full tensor of linear elasticity, which includes the major term of the linear elasticity of the undoped crystal and the doping-induced correction $\hat{\Lambda}_2$.

An important feature of the relative shift $\delta\omega_\nu/\omega_\nu$ is its scaling with the size of the system. The vibration amplitude A_ν in Eq. (10) can be scaled by the lateral dimension L , for example the length of a nanobeam or a nanowire for an extension mode, or the size of the square for a Lamé mode, or the diameter of a disk for a breathing mode in a disk. Respectively, we write $A_\nu = \eta_\nu L$. Then, if one takes into account the explicit form (8) of the parameter $\gamma_\nu = \gamma_{\nu\nu\nu\nu}^{(e)}$, one finds from Eq. (10) that the ratio $\delta\omega_\nu/(\eta_\nu^2 \omega_\nu)$ is independent of the system size for the aforementioned modes. In this estimate we used that the tensors $\hat{\Lambda}$ are material parameters and are independent of the geometry. We also used that modes of interest have typical wavelength $\sim L$, therefore $\hat{\varepsilon}^{(\nu)}$ scales as L^{-1} .

Most of the experiments in nano- and micromechanics are done with nanobeams, nanowires, membranes, or thin plates. In such systems the thickness is much smaller than the length or, in the case of membranes or plates, the lateral dimensions. Then, from the boundary condition of the absence of tangential stress on free surfaces [21], it follows that the strain tensor $\hat{\varepsilon}$ weakly depends on the coordinate normal to the surface. This simplifies the denominator in Eq. (10), making it proportional to the thickness. Similarly, from Eq. (8) γ_ν is also proportional to the thickness, and the thickness drops out of Eq. (10). The explicit expressions for $M\omega_\nu^2$ and γ_ν that determine the denominator and the numerator in Eq. (10), respectively, are given in Appendices C and D for Lamé and extension modes. These expressions are cumbersome, and it is convenient to use symbolic programming to obtain them. [27]

A. Temperature and Electron Density Dependence of the Scaled Nonlinear Frequency Shift

The scaled ratio $\delta\omega_\nu/(\eta_\nu^2\omega_\nu)$ that characterizes the relative nonlinear frequency shift is shown in Figure 1 for several modes that are often used in single-crystal silicon MEMS. This ratio depends on the type of the mode and the crystal orientation. Figure 1 refers to high-symmetry crystal orientations, in which case the modes have a comparatively simple spatial structure and the surfaces can be made smooth. We used the values $\Xi_u = 8.8$ eV [28], $\Xi_{sh} = 300$ eV, the effective mass for density of states $m_{eff} = 0.32m_e$ [29], and the temperature-dependent linear elasticity parameters given in Ref. [30].

Figure 1 shows that the electron-redistribution induced nonlinearity of vibrational modes is very strong. For the ratio of the vibration amplitude to the system size $\eta \sim 10^{-4}$ and the mode eigenfrequency $\omega_\nu/2\pi \sim 10$ MHz, the frequency change can be as large as $\delta\omega_\nu/2\pi \sim 0.1$ kHz. This explains, qualitatively, the observations [17]. A quantitative comparison with the experiment [17] is complicated, as the observations refer to different samples. Our preliminary results show an excellent quantitative agreement with the data obtained for the same sample at different temperatures and for different types of modes [31].

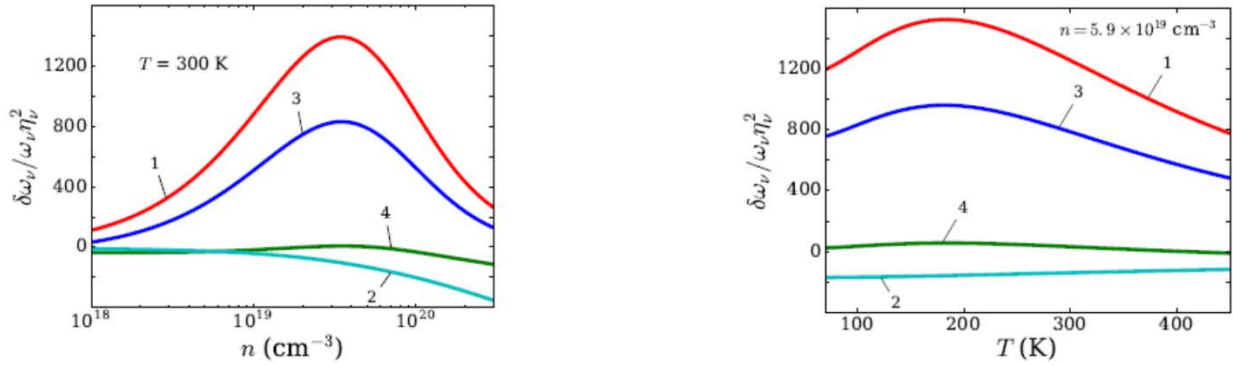


FIGURE 1. Relative change $\delta\omega_\nu/\omega_\nu$ of the vibration frequency of a mode with the vibration amplitude η_ν , scaled by the relevant size of the system, cf. Eq. (10). The results refer to single crystal silicon resonators. Curves 1 and 2 refer to the first Lamé mode in square plates cut in $\langle 100 \rangle$ and $\langle 110 \rangle$ directions, respectively. In this case, the size of the resonator is the length of the side of the square. Curves 3 and 4 refer to the first extension mode in beams cut in $\langle 100 \rangle$ and $\langle 110 \rangle$ directions, respectively. In this case, the size of the resonator is the length of the beam.

The nonlinear frequency shift displays several characteristic features, as seen from Figure 1. One of them is the strong dependence of the shift on the type of the mode and the crystal orientation. For both the Lamé and the extension mode, the shift is much stronger for crystals cut out in $\langle 100 \rangle$ direction than in $\langle 110 \rangle$ direction. This is a consequence of the electron energy valleys lying along the $\langle 100 \rangle$ axes, making the system more “responsive” to the lattice displacement along these axes. Interestingly, in the both configurations the shifts for the Lamé modes are larger than for the extension modes.

A somewhat unexpected feature is the nonmonotonic dependence of the nonlinear frequency shift on the electron density and temperature. The nonmonotonicity occurs in the range where the electron system is close to degeneracy, $\mu_0/k_B T \sim 1$, and it strongly depends on the crystal orientation. It is much stronger for crystals cut in $\langle 100 \rangle$ than $\langle 110 \rangle$ directions. For a crystal cut in $\langle 110 \rangle$ direction, both the density and temperature dependence of the shift are monotonic in the case of the Lamé mode, whereas for the extension mode the nonmonotonicity is weak.

The nonmonotonicity of the frequency shift stems from the behavior of the parameters $nC_{2,3,4}$ in the range $\mu_0 \sim k_B T$. As seen from Table I, parameter nC_2 exponentially increases with the increasing $\mu_0/k_B T$ for negative $\mu_0/k_B T$, but for large positive $\mu_0/k_B T$ it falls off $\mu_0/k_B T^{-3/2}$. It has a pronounced maximum for $\mu_0/k_B T \approx 0.6$. Parameter nC_3 also displays a maximum, which occurs for $\mu_0/k_B T \approx 1.1$. In contrast, parameters $nC_{1,4}$ depend on $\mu_0/k_B T$ monotonically.

The results of Appendices C and D show that, for the Lamé and extension modes in crystals cut in $\langle 100 \rangle$ direction, the relative shift $\delta\omega_v/\omega_v$ is determined by coefficient nC_2 , which explains the nonmonotonicity of the shift. For crystals cut in $\langle 110 \rangle$, the shift of the Lamé mode is fully determined by coefficient nC_4 and is monotonic, whereas for the extension mode the expression for the shift has contributions from nC_2 , nC_3 , and nC_4 that partly compensate each other, leading to a comparatively small shift all together and its weak nonmonotonicity.

IV. Conclusions

The results of this paper show that the electron-phonon coupling strongly affects the nonlinearity of vibrational modes in semiconductor-based nano- and micromechanical systems. The mechanism of the effect is the strain-induced redistribution of the electrons between the valleys of the conduction band. The redistribution results from lifting the degeneracy of the electron energy spectrum by the strain from a vibrational mode. The analysis refers to the range of temperatures where the rate of intervalley scattering strongly exceeds the frequencies of the considered modes. In this case the valley populations follow the strain adiabatically.

The change of the valley populations is a strongly nonlinear function of the strain tensor. The respective expansion of the free energy in the strain is an expansion in the strain multiplied by the ratio of the electron-phonon coupling energy (in particular, the deformation potential) to the chemical potential of the electron system or the temperature. This ratio is large, $\gtrsim 10^3$. It is this parameter that makes the nonlinearity of the vibrational modes in doped semiconductor structures strong.

Of special interest in nano- and micromechanical systems is the amplitude dependence of the vibration frequency. To the leading order, it is determined by the quartic terms in the expansion of the free energy in strain. These terms are comparatively large in doped crystals. We have calculated the nonlinear elasticity tensor that describes the electron contribution to the terms in the free energy, which are quartic in the strain. The explicit expressions for the tensor components refer to semiconductors with the valleys on $\langle 100 \rangle$ axes, in particular, to silicon. We have also found this tensor for germanium. In silicon, along with the deformation potential coupling, an important role is played by the coupling to shear strain. Such strain lifts the band

degeneracy at the zone boundary and is effectively described by a two-phonon coupling. We show that this coupling also leads to strong nonlinearity of vibrational modes.

The parameter of the electron coupling to shear strain in silicon is not easy to access in the experiment [26, 32]. Measurements of the nonlinear frequency shift provide a direct means for determining this parameter. In particular, the nonlinear frequency shift of the fundamental Lamé mode in a silicon plate cut along $\langle 110 \rangle$ axes is determined by this parameter only, except for small corrections from the nonlinearity of the undoped crystal.

We found that the nonlinear frequency shift strongly depends on the type of a vibrational mode and the crystal orientation. We also found that the ratio of the frequency shift to the squared vibration amplitude can be profoundly nonmonotonic as a function of electron density and temperature. The results provide an insight into the experimentally observed strong mode nonlinearity in doped crystals [17]. In terms of applications, they enable choosing the appropriate range of doping and the temperature regime to optimize the operation of nano- and micromechanical resonators.

Acknowledgements

We are grateful to T. Kenny for attracting our attention to the problem and for stimulating discussions. We benefited from useful discussions with J. Atalaya, D. Heinz, P. Polunin, S. W. Shaw, and Y. Yang. This research was supported in part by the US Defense Advanced Research Projects Agency (Grant No. FA8650-16-1-7600).

Appendix A: Expansion of the Free Energy in Terms of the Strain-Induced Shift of the Energy Valleys

The major effect of a strain on the electron free energy comes from the shift of the energy valleys. We will assume that valley α is shifted in energy by δE_α and the shift is small, $|\delta E_\alpha| \ll \max(k_B T, \mu_0)$, where μ_0 is the chemical potential in the absence of strain. We further assume that the vibrations are slow compared to the time it takes the electron system to come, locally, to thermal equilibrium for given values of δE_α , i.e., the temperature and the chemical potential are the same in all valleys. Since for high electron densities the thermal conductivity is high, the change of the temperature compared to the ambient temperature can be disregarded; also, as mentioned in the main text, the electron density n summed over all valleys is constant.

Expanding the electron free energy density to the 4th order in the strain-induced shifts δE_α , we find that, in an N -valley semiconductor, the change δF_e of the free energy density is

$$\begin{aligned} \frac{\delta F_e}{nk_B T} = & \bar{\Delta}_\epsilon + \frac{1}{2} \frac{F'_{1/2}}{F_{1/2}} \left[(\overline{\Delta_\epsilon})^2 - \overline{\Delta_\epsilon^2} \right] + \frac{1}{6} \frac{F''_{1/2}}{F_{1/2}} \left[\overline{\Delta_\epsilon^3} - 3\overline{\Delta_\epsilon^2} \overline{\Delta_\epsilon} + 2(\overline{\Delta_\epsilon})^3 \right] \\ & + \frac{1}{8} \frac{F'''_{1/2}}{F_{1/2} F'_{1/2}} \left[(\overline{\Delta_\epsilon^2})^2 - 2\overline{\Delta_\epsilon^2} (\overline{\Delta_\epsilon})^2 + (\overline{\Delta_\epsilon})^4 \right] + \frac{1}{24} \frac{F''''_{1/2}}{F_{1/2}} \left[4\overline{\Delta_\epsilon^3} \overline{\Delta_\epsilon} - \overline{\Delta_\epsilon^4} - 6\overline{\Delta_\epsilon^2} (\overline{\Delta_\epsilon})^2 + 3(\overline{\Delta_\epsilon})^4 \right]. \end{aligned} \quad (\text{A1})$$

Here, $\overline{\Delta_\varepsilon^m} = N^{-1} \sum_\alpha (\delta E_\alpha / k_B T)^m$. We use the standard notation

$F_{1/2}(x) = \int_0^\infty dy y^{1/2} / [1 + \exp(y - x)]$ primes $dF_{1/2}/dx$. Function $F_{1/2}$ and its derivatives are calculated for $x = \mu_0 / k_B T$.

Equation (A1) immediately gives the tensors $\widehat{\Lambda}_n$ of the expansion of the free energy increment (6) if one expresses the shift δE_α of the valleys in terms of the strain tensor. In the deformation potential approximation the relation between δE_α and ε^\wedge is given in the main text, see also Eq. (A2) below.

In the case of Si crystals, which are often used in micromechanical resonators, an important contribution to δE_α comes from the shear-strain induced splitting of the electron energy bands at the zone boundary. Shear strain does not lead to the valley shift in the deformation potential approximation. The overall shift of valley α , to the lowest order in the coupling that causes it (i.e., to the first order in the deformation potential where its contribution is nonzero and to the second order in the band splitting for shear strain) is [26]:

$$\delta E_\alpha = \sum_{ij} \Xi_{ij}^{(\alpha)} \varepsilon_{ij} - \Xi_{\text{sh}} \varepsilon_\alpha^2, \quad \Xi_{\text{sh}} = \frac{4\Xi_{u'}^2}{\Delta E}. \quad (\text{A2})$$

Here we use that silicon has six valleys located at the $\langle 100 \rangle$ axes, and we chose the coordinate axes x, y, z along $\langle 100 \rangle$. Respectively, the valley index α takes on three values that correspond to the x, y, z axes (the valleys lying on the same axis, but in the opposite directions, are equivalent). The strain ε_α , which enters the second term in the right-hand side of Eq. (A2), is a component of the strain tensor ε_{ij} with i, j such that $i, j \neq \alpha$ and $i \neq j$. The parameter $2\Xi_{u'}$ is the interband matrix element of the electron-phonon coupling calculated for the electron conduction bands Δ_1 and Δ_2' at the X point on the boundary of the Brillouin zone, where the bands cross; ΔE is the energy separation between the bands Δ_1 and Δ_2' at the value of the wave vector \mathbf{k} that corresponds to the conduction band minimum. Parameter Ξ_{sh} is the effective deformation potential of two-phonon coupling to shear strain. The numerical value of Ξ_{sh} is not well known. The experimental data give $\Xi_{u'} \approx 7 - 8$ eV [26, 32] and the numerical data on the band splitting give $\Delta E \approx 0.7$ eV [33] so that Ξ_{sh} is in the range of 280 – 360 eV; this is essentially an order of magnitude estimate.

In calculating δF_e in Eq. (A1) we kept terms that are quartic in ε^\wedge . The components of the tensors $\widehat{\Lambda}_k$ in Eq. (6) are expressed in terms of δF_e as

$$(\Lambda_k)_{i_1 j_1 \dots i_k j_k} = \frac{\partial^k \delta F_e}{\partial \varepsilon_{i_1 j_1} \dots \partial \varepsilon_{i_k j_k}}. \quad (\text{A3})$$

Tensors $\widehat{\Lambda}$ are symmetric with respect to the interchange of indices $i_k \leftrightarrow j_k$ and the pairs $(i_k j_k) \leftrightarrow (i_k' j_k')$. For the considered long-wavelength strain, tensors $\widehat{\Lambda}_k$ are independent of coordinates. The corrections $\widehat{\Lambda}_2$ to the linear elasticity tensors were found previously [19, 20] and are not discussed in this paper.

Appendix B: Nonlinear Elastic Constants of Germanium

In this section we provide the corrections to the nonlinear elastic constants of germanium, which are due to the redistribution of the electrons over the valleys. Germanium has four equivalent valleys in the conduction band, which are located on the boundary of the Brillouin zone along $\langle 111 \rangle$ axes. We use the Voigt notation and write the components of the corrections to the nonlinear elasticity tensor $\delta\hat{c}$ in the frame where the axes (x, y, z) are along the $\langle 100 \rangle$ directions of the crystal. Using the results of Appendix A, we obtain

$$\begin{aligned}\delta c_{456} &= \frac{n\Xi_u^3 F''_{1/2}}{27F_{1/2}(k_B T)^2}, \\ \delta c_{4444} &= \frac{n\Xi_u^4}{81(k_B T)^3} \left(\frac{3(F''_{1/2})^2}{F_{1/2}F'_{1/2}} - \frac{F'''_{1/2}}{F_{1/2}} \right), \\ \delta c_{4455} &= \frac{n\Xi_u^4}{81(k_B T)^3} \left(\frac{(F''_{1/2})^2}{F_{1/2}F'_{1/2}} - \frac{F'''_{1/2}}{F_{1/2}} \right).\end{aligned}\quad (\text{B1})$$

The notations are the same as in Appendix A and in Table I. The electron-phonon coupling does not contribute to the other third- and fourth-order elastic constants.

Corrections δc_{44} and δc_{456} for germanium were found by Keyes [18]; however, his final expression for δc_{456} differs from Eq. (B1) by a factor of 4 (our expressions for δc_{44} coincide with Ref. [18]). Parameters δc_{4444} and δc_{4455} have not been found before, to the best of our knowledge. In the limiting cases, corrections δc_{4444} and δc_{4455} have the same dependence on temperature and electron density as constant nC_2 discussed in Sec. IV A.

Appendix C: Duffing Nonlinearity Parameter for a Lamé Mode in a Square Single-Crystal Plate

We consider a square plate with side L and thickness h made out of a single crystal with cubic symmetry. If the crystal is cut out along $\langle 100 \rangle$ or $\langle 110 \rangle$ axes, one of the simplest modes is the first Lamé mode [34]. The normalized displacement field is

$$\begin{aligned}u_x^{(\nu)} &= \sqrt{2} \cos(\pi x/L) \sin(\pi y/L), \\ u_y^{(\nu)} &= -\sqrt{2} \sin(\pi x/L) \cos(\pi y/L).\end{aligned}\quad (\text{C1})$$

Here, x and y axes are in the lateral plane along the sides of the square, axis z is perpendicular to the plate and $u_z^{(\nu)} = 0$. Calculating the strain tensor for the displacement (C1) and substituting the expressions into Eqs. (8) and the relation

$$M\omega_\nu^2 = \int d\mathbf{r} \hat{\Lambda}_2^{(f)} \cdot \hat{\epsilon}^{(\nu)} \otimes \hat{\epsilon}^{(\nu)}, \quad (\text{C2})$$

for the plate cut out along $\langle 100 \rangle$ axes we obtain, in Voigt notation for the elasticity tensors,

$$\begin{aligned} M\omega_\nu^2 &= \pi^2 h (c_{11} - c_{12}), \\ \gamma_\nu &= \frac{3\pi^4 h}{16L^2} (c_{1111} - 4c_{1112} + 3c_{1122}). \end{aligned} \quad (\text{C3})$$

If we consider silicon and take into account only the contribution δc^\wedge to the nonlinear elasticity tensor c^\wedge , with the account taken of Table I, the expression for γ_ν simplifies to

$$\gamma_\nu = (27\pi^4 h / 32L^2) \delta c_{1111}. \quad (\text{C4})$$

For the Lamé mode cut along the $\langle 110 \rangle$ axis, if the tensors are calculated in the axes $\langle 100 \rangle$, we have

$$\begin{aligned} M\omega_\nu^2 &= 2\pi^2 h c_{44}, \\ \gamma_\nu &= (3\pi^4 h / 2L^2) \delta c_{4444}. \end{aligned} \quad (\text{C5})$$

Note that only coupling to shear strain contributes to the nonlinearity parameter γ_ν in this case.

Appendix D: Duffing Nonlinearity Parameter for an Extension Mode in a Single-Crystal Narrow Beam

We consider the fundamental extension mode in a thin beam of length L with a rectangular cross-section of area $S \ll L^2$. The beam is cut along a symmetry axis, and the sides are also along symmetry planes of a cubic crystal. From the free-surface boundary conditions, the normalized displacement field is [34]:

$$\begin{aligned} u_x^{(\nu)} &\approx \sqrt{2} \cos(\pi x / L), \\ u_y^{(\nu)} &\approx \frac{\sqrt{2}\pi\sigma_2}{L} y \sin(\pi x / L), \\ u_z^{(\nu)} &\approx \frac{\sqrt{2}\pi\sigma_3}{L} z \sin(\pi x / L). \end{aligned} \quad (\text{D1})$$

This expression takes into account transverse compression that accompanies beam extension and uses the smallness of the beam cross-section; corrections $\sim S/L^2$ are disregarded. The transverse compression in a cubic crystal cut in a symmetric direction is described by Poisson's ratios σ_2 and σ_3 . Generally, they do not coincide. In Eq. (D1) the transverse coordinates y and z are counted off from the center of the beam

For the longitudinal direction of the beam $\langle 100 \rangle$ and the sides parallel to (100) planes, the Poisson parameters are equal, $\sigma_2 = \sigma_3$ and $\sigma \equiv \sigma_2 = \sigma_3 = c_{12}/(c_{11} + c_{12})$. In this case Eqs. (8) and (C2) give

$$\begin{aligned}
M\omega_\nu^2 &= \frac{\pi^2 S (c_{11} (c_{11} + c_{12}) - 2c_{12}^2)}{L (c_{11} + c_{12})}, \\
\gamma_\nu &= (\pi^4 S/4L^3) [c_{1111} - 8\sigma c_{1112} \\
&\quad + 12\sigma^2 (c_{1122} + c_{1123}) - 8\sigma^3 (c_{1112} + 3c_{1123}) \\
&\quad + 2\sigma^4 (c_{1111} + 4c_{1112} + 3c_{1122})]. \quad (D2)
\end{aligned}$$

The expression for γ_ν is simplified if in the nonlinear elasticity tensors we take into account only the contribution from the electron-phonon coupling as given in Table I and also allow for the interrelation between different components of the tensor $\delta\hat{c}$. Then for a silicon beam

$$\gamma_\nu = (\pi^4 S/4L^3)(1 + \sigma)^4 \delta c_{1111}. \quad (D3)$$

For extension along $\langle 110 \rangle$ axis, with one side parallel to (100) plane and the other side parallel to $(1\bar{1}0)$ plane, the Poisson's ratios $\sigma_2 = \sigma(110, 1\bar{1}0)$ and $\sigma_3 = \sigma(110, 001)$ are given in Ref. [35]. Then Eqs. (8) and (C2) give

$$\begin{aligned}
M\omega_\nu^2 &= \frac{4\pi^2 S}{L} \frac{c_{44} (c_{11}(c_{11} + c_{12}) - 2c_{12}^2)}{c_{11}(c_{11} + c_{12} + 2c_{44}) - 2c_{12}^2}, \\
\gamma_\nu &= \frac{\pi^4 S}{32L^3} \left[c_{1111} (\sigma_2^4 - 4\sigma_2^3 + 6\sigma_2^2 - 4\sigma_2 + 8\sigma_3^4 + 1) \right. \\
&\quad + 4c_{1112} (\sigma_2 - 1) (\sigma_2^3 + 2\sigma_2^2\sigma_3 - 3\sigma_2^2 - 4\sigma_2\sigma_3 + 3\sigma_2 + 8\sigma_3^3 + 2\sigma_3 - 1) \\
&\quad + 3c_{1122} (\sigma_2 - 1)^2 (\sigma_2^2 - 2\sigma_2 + 8\sigma_3^2 + 1) + 24c_{1123}\sigma_3 (\sigma_2 - 1)^2 (\sigma_2 + \sigma_3 - 1) \\
&\quad + 48c_{1144}\sigma_3^2 (\sigma_2 + 1)^2 + 96c_{1244}\sigma_3 (\sigma_2 - 1) (\sigma_2 + 1)^2 + 24c_{1155} (\sigma_2^2 - 1)^2 \\
&\quad \left. + 24c_{1266} (\sigma_2^2 - 1)^2 + 8c_{4444} (\sigma_2 + 1)^4 \right]. \quad (D4)
\end{aligned}$$

If in the nonlinear elasticity tensor \hat{c} we take into account only the contribution $\delta\hat{c}$ from the electron-phonon coupling, in the case of a silicon beam the expression for γ_ν simplifies to

$$\gamma_\nu = \frac{\pi^4 S}{32L^3} \left((\sigma_2 - 2\sigma_3 - 1)^4 \delta c_{1111} + 24 (\sigma_2 + 1)^2 (\sigma_2 - 2\sigma_3 - 1)^2 \delta c_{1144} + 16 (\sigma_2 + 1)^4 \delta c_{4444} \right). \quad (D5)$$

Expressions (D2) and (D4) were generated using a computer code to calculate the sums and integrals in Eq. (8).

- [1] D. Fedorets, L. Y. Gorelik, R. I. Shekhter, and M. Jonson, *Phys. Rev. Lett.* **92** (2004), 10.1103/Phys-RevLett.92.166801.
- [2] N. M. Chtchelkatchev, W. Belzig, and C. Bruder, *Phys. Rev. B* **70**, 193305 (2004).
- [3] J. Koch, M. E. Raikh, and F. von Oppen, *Phys. Rev. Lett.* **95**, 056801 (2005).
- [4] F. Pistolesi and S. Labarthe, *Physical Review B* **76**, 165317 (2007).
- [5] O. Usmani, Y. M. Blanter, and Y. V. Nazarov, *Phys. Rev. B* **75**, 195312 (2007).
- [6] R. Leturcq, C. Stampfer, K. Inderbitzin, L. Durrer, C. Hierold, E. Mariani, M. G. Schultz, F. von Oppen, and K. Ensslin, *Nat. Phys* **5**, 327 (2009).
- [7] G. A. Steele, A. K. Huttel, B. Witkamp, M. Poot, H. B. Meerwaldt, L. P. Kouwenhoven, and H. S. J. van der Zant, *Science* **325**, 1103 (2009).
- [8] B. Lassagne, Y. Tarakanov, J. Kinaret, D. Garcia-Sanchez, and A. Bachtold, *Science* **325**, 1107 (2009).
- [9] M. N. Kiselev, K. A. Kikoin, L. Y. Gorelik, and R. I. Shekhter, *Physical Review Letters* **110**, 066804 (2013).
- [10] A. N. Cleland, *Foundations of nanomechanics: from solid-state theory to device applications* (Springer, Berlin, 2003).
- [11] R. Lifshitz and M. C. Cross, in *Review of Nonlinear Dynamics and Complexity*, edited by H. G. Schuster (Wiley, Weinheim, 2008) pp. 1–52.
- [12] H.-Y. Hao and H. J. Maris, *Phys. Rev. B* **64**, 064302 (2001).
- [13] A. V. Akimov, A. V. Scherbakov, P. J. S. van Capel, J. I. Dijkhuis, T. Berstermann, D. R. Yakovlev, and M. Bayer, *J. Phys. Conference Series* **92**, 012002 (2007).
- [14] S. Ghaffari, S. A. Chandorkar, S. S. Wang, E. J. Ng, C. H. Ahn, V. Hong, Y. S. Yang, and T. W. Kenny, *Scientific Reports* **3**, 3244 (2013).
- [15] M. Sansa, E. Sage, E. C. Bullard, M. Gely, T. Alava, E. Colinet, A. K. Naik, G. L. Villanueva, L. Duraffourg, M. L. Roukes, G. Jourdan, and S. Hentz, *Nat. Nanotech.* **11**, 552 (2016).
- [16] M. Shahmohammadi, H. Fatemi, and R. Abdolvand, in *IEEE 26th International Conference on Micro Electro Mechanical Systems* (2013) pp. 793–796.
- [17] Y. Yang, E. J. Ng, P. M. Polunin, Y. Chen, I. B. Flader, S. W. Shaw, M. I. Dykman, and T. W. Kenny, *IEEE Journal of Microelectromechanical Systems* **25**, 859 (2016).
- [18] R. Keyes, *IBM Journal of Research and Development* **5**, 266 (1961).
- [19] J. J. Hall, *Phys. Rev.* **161**, 756 (1967).
- [20] F. Cerdeira and M. Cardona, *Physical Review B* **5**, 1440 (1972).
- [21] L. Landau and E. Lifshitz, *Theory of elasticity*, 3rd ed. (Butterworth-Heinemann Ltd., Oxford, 1986).
- [22] L. D. Landau and E. M. Lifshitz, *Mechanics*, 3rd ed. (Elsevier, Amsterdam, 2004).
- [23] M. I. Dykman and M. A. Krivoglaz, *JETP* **37**, 506 (1973).
- [24] E. J. Ng, V. Hong, Y. Yang, C. H. Ahn, C. L. M. Evenhart, and T. W. Kenny, *JMEMS* **24**, 730 (2015).
- [25] G. L. Bir and G. E. Pikus, *Symmetry and Strain-induced Effects in Semiconductors* (Wiley, N.-Y., 1974).
- [26] J. C. Hensel, H. Hasegawa, and M. Nakayama, *Physical Review* **138**, A225 (1965).
- [27] The program that performs the analytical calculations and evaluates the numerical values of the parameters is available at <http://www.pa.msu.edu/people/dykman/nonlinear-elasticity>.
- [28] P. Y. Yu and M. Cardona, *Fundamentals of Semiconductors* (Springer, Berlin, 2001).
- [29] J. Hensel, H. Hasegawa, and M. Nakayama, *Physical Review* **138**, A225 (1965).
- [30] Y. P. Varshni, *Phys. Rev. B* **2**, 3952 (1970).
- [31] D. Heinz, K. Moskovtsev, and T. W. Kenny, in preparation (2016).
- [32] L. D. Laude, F. H. Pollak, and M. Cardona, *Physical Review B* **3**, 2623 (1971).
- [33] B. D. Malone and M. L. Cohen, *J. Phys. C* **25**, 105503 (2013).
- [34] K. F. Graff, *Wave Motion in Elastic Solids* (Dover Publications, New York, 1991).
- [35] R. H. Baughman, J. M. Shacklette, A. A. Zakhidov, and S. Stafstrom, *Nature* **392**, 362 (1998).

LIST OF ACRONYMS, ABBREVIATIONS, AND SYMBOLS

ACRONYM	DESCRIPTION
AFRL	Air Force Research Laboratory
DARPA	Defense Advanced Research Agency
Ge	Germanium
MEMS	Microelectromechanical Systems
Si	Silicon